FLOQUET WAVE DIFFRACTION AT THE EDGE OF AN ARRAY OF PRINTED DIPOLES

A. Polemi, A. Toccafondi, S. Maci

Department of Information Engineering, University of Siena,
Via Roma 56, 53100 Siena Italy,
E-mail: albertot@ing.unisi.it; polemale@dii.unisi.it; macis@ing.unisi.it

INTRODUCTION

Printed antenna array technology is becoming increasingly popular for its well known advantages. The electromagnetic modeling of these antennas is often based on the hypothesis of infinite structure that allows the reduction of the numerical effort to that for solving a single cell of periodicity, by expanding the field quantities in terms of Floquet waves (FW).

The basic constituent of an efficient full-wave analysis of printed arrays is the array Green's function (AGF). This latter may be represented as the field radiated by an array of electric dipoles located on an infinite grounded dielectric slab, which is globally excited with the same amplitude and phase of the actual array. The efficient representation of the AGF, which is extremely convenient with respect to the summation of individual dipole contributions, is the radiation from a superposition of continuous equivalent FW source distribution extending over the finite array aperture. The asymptotic treatment of each FW aperture distribution leads to a spatially truncated version of the infinite array FW expansion, plus FW-modulated diffracted contributions from the edges and vertexes of the array. The free-space standing AGF has been treated in [2] and [3] for edge and vertex Floquet induced diffracted rays, respectively. In this paper, the formulation in [2] has been extended to the case of dipoles on a grounded dielectric slab, and applied to the case of a strip array. This configuration has been considered for the fact that the AGF is produced by only edge-diffracted rays; vertex diffracted rays, which allows extension to rectangular array, are presently under investigation.

FORMULATION

The geometry of the structure is presented in Fig. 1. A strip array of phased elementary dipoles is placed on a grounded dielectric substrate of thickness h and relative permittivity ϵ_r. A rectangular reference system (x, y, z) is introduced with the z-axis perpendicular to the grounded slab and the y-axis along one of the two edges of the strip array. A spherical coordinate system (r, θ, ϕ) is also defined. The interelement period is denoted by d_x along the x-axis, and d_y along the y-axis, while the linear phasing between the element is $k_{x0}d_x$ and $k_{y0}d_y$ respectively. Let us suppose the strip array be infinitely extended in the y-direction and characterized by a width $w = Nd_x$, where N is the number of the elementary dipoles in the x direction. In the following we will also assume that $k_{x0}^2 + k_{y0}^2 < k^2$, so that the array radiation exhibits maximum in the direction $\hat{s} = \frac{1}{k}(k_{x0}\hat{x} + k_{y0}\hat{y} - \sqrt{k^2 - k_{x0}^2 - k_{y0}^2}\hat{z})$. The high-

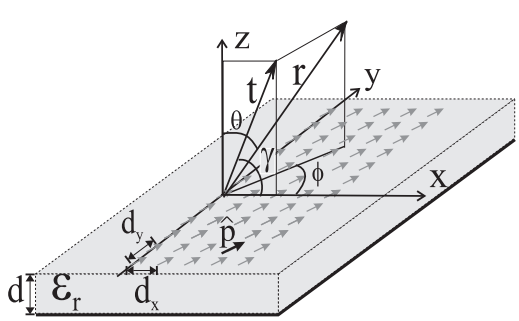

Fig. 1. Geometry of the structure

frequency description of the field radiated by the strip can be based directly on the solution for the

canonical problem of a semi-infinite array of dipoles printed on a grounded slab. To this end let us denote with $\mathbf{E}(P, x')$ the electric field at $P = (x, y, z)$ radiated by an array with semi-infinite extension in the x-direction and with the edge located at x'. By cancellation, the radiated field $\mathbf{E}^{st}(P)$ by the strip may be represented as $\mathbf{E}^{st}(P) = \mathbf{E}(P; 0) - \mathbf{E}(P; Nd_x)$; as a consequence we only need to derive a suitable high-frequency expression for $\mathbf{E}(P; x')$. A general expression of $\mathbf{E}(P; x')$ may be obtained as an element by element summation of the dielectric field radiated by a single dipole on a grounded dielectric slab This latter field may be expressed as in [5] as a plane wave spectral integral form involving the spectral dyadic Green's function $\underline{\underline{\mathbf{G}}}$. The double spatial summation expressing the total radiated field by the semi-infinite array, exhibits a very poor convergence properties, especially when the observation point is far removed from the edge of the array. This drawback can be overcome interchanging the order of summation and integration, and restructuring the expression by using the Poisson summation formula [2] thus leading to

$$\mathbf{E}(P; x') = \frac{1}{2\pi d_y} \sum_{q=-\infty}^{\infty} \int_{-\infty}^{\infty} B(k_x) \underline{\underline{\mathbf{G}}}(\mathbf{k}_q) \cdot \hat{p} e^{-j\mathbf{k}_q \cdot \mathbf{r}} \mathrm{d}k_x \tag{1}$$

where $\mathbf{k}_q = k_x \hat{x} + k_{yq} \hat{y} + k_{zq} \hat{z}$ with $k_{zq} = \sqrt{k^2 - k_x^2 - k_{yq}^2}$ and $\hat{p} = p_x \hat{x} + p_y \hat{y}$ is the unit vector denoting the direction of the dipoles. The q-sum of the above expression represents the Floquet-wave expansion of the field along the infinite periodic y-domain, whose wavenumbers are defined as $k_{yq} = k_{y0} + \frac{2\pi q}{d_y}$ $(q = 0, \pm 1, \ldots)$. The function $B(k_x) = [1 - e^{j(k_x - k_{x0})d_x}]^{-1}$ exhibits real poles located on the real k_x-axis at $k_{xp} = k_{x0} + \frac{2\pi p}{d_y}$ $(p = 0, \pm 1, \ldots)$ which defines the Floquet wave (FW) wavenumbers along the semi-infinite periodic x-axis. The residue contributions of the integrand in (1) associated to those FW poles located on the proper Riemann sheet ($Im(k_{zq}) < 0$) represent propagating (real k_{zpq}) or evanescent (imaginary k_{zpq}) FWs associated to the infinite array. Furthermore, the spectral dyadic Green's function $\underline{\underline{\mathbf{G}}}(\mathbf{k}_q)$ may exhibit real and complex poles. The residues of the integrand in (1) at these poles correspond to surface waves (SW) and leaky waves (LW), excited at the array edge.

UNIFORM ASYMPTOTIC SOLUTION

In order to perform an asymptotic evaluation of the integral (1) the original contour k_x is deformed on the steepest descendant path (SDP) relevant to the saddle point. In this deformation FW, SW, or LW poles may be captured, so that their residue contributions have to be included, thus leading to

$$\mathbf{E}(P) = \sum_q \mathbf{E}_q^d + \sum_{p,q} \mathbf{E}_{pq}^{FW} U(\gamma_{pq}^{SB} - \gamma) + \sum_{i,q} \mathbf{E}_{iq}^{SW/LW} U(\gamma_{iq}^{SB} - \gamma) \tag{2}$$

where $\mathbf{E}_q^d$ represents the integration on the SDP, and the other terms of the summation are the residues of the integrand in (1). This, multiplied by Heavyside unit step function U(η) ($U(\eta) = 1 \quad \text{for} \quad \eta > 0, U(\eta) = 0 \quad \text{for} \quad \eta < 0$), terminates the domain of existence of the various waves at pertinent shadow boundary planes (SBP). These SBP are defined to occur at the observation angle $\gamma = \gamma_{pq}^{SB}$ and $\gamma = \gamma_{iq}^{SB}$ for which the FW poles and SW/LW poles cross the SDP. The edge diffraction mechanism and the related SB angles for FWs and SWs are depicted in Fig. 2 and 3, respectively. In particular, Fig. 2 shows the edge diffracted rays induced by q-indexed FWs for the case of phase velocity along the edge greater than the speed of light ($|k_{yq}| < k$) (Fig. 2a) and less than the speed of light ($|k_{yq}| > k$) (Fig. 2b). The shadow boundary planes are also depicted. Fig. 3 shows the edge diffraction associated to the guided waves. Let us denote by k_{zi} the z-component of the complex wavenumber which corresponds to the solution of the slab dispersion equation. Surface wave poles are those corresponding to k_{ziq} purely imaginary, and leaky wave poles correspond to complex k_{zi}. In Fig. 3a the angle η_{iq}^{SW} between the real (propagating) part of the SW vector wavenumber and the edge is such to maintain the projection of such a vector along $\hat{y}$ equal to $k_{yq} < \sqrt{k^2 + |k_{zi}|^2}$; then $\eta_{iq}^{SW} = \cos^{-1}\left(k_{yq} / \sqrt{k^2 + |k_{zi}|^2}\right)$. When q (or frequency) is such as $k_{yq} > \sqrt{k^2 + |k_{zi}|^2}$, the surface wave becomes exponentially attenuated along $\hat{t}$ similarly as it happens for Fig. 2b. In Fig. 3b, the various geometrical quantities are depicted, which are related to the direction of the real and imaginary part of each edge diffracted LW vector wavenumber. The

real part of the complex vector wavenumber k_{iq}^{LW} propagates in a direction characterized by the angles θ_{iq}^{LW} w.r.t. $\hat{z}$ and η_{iq}^{LW} w.r.t. $\hat{y}$. These two angles are related to k_{yq} by $\eta_{iq}^{LW} = \cos^{-1}\left(k_{yq}/Re\{\mathbf{k}_{iq}^{LW}\}\right)$ and $\theta_{iq}^{LW} = Re\{k_{zi}\}/|Re\{\mathbf{k}_{iq}^{LW}\}|$. The imaginary part of $\mathbf{k}_{iq}^{LW}$ is orthogonal to $Re\{\mathbf{k}_{iq}^{LW}\}$ in order to satisfy the free-space plane-wave dispersion equation $\mathbf{k}_{iq}^{LW} \cdot \mathbf{k}_{iq}^{LW} = k^2$. Furthermore, $Im\{\mathbf{k}_{iq}^{LW}\}$ is orthogonal to $\hat{y}$, and forms with $\hat{z}$ the angle $\delta_{iq}^{LW} = Im\{k_{ziq}^{LW}\}/|Im\{k_{ziq}^{LW}\}|$ In order to obtain

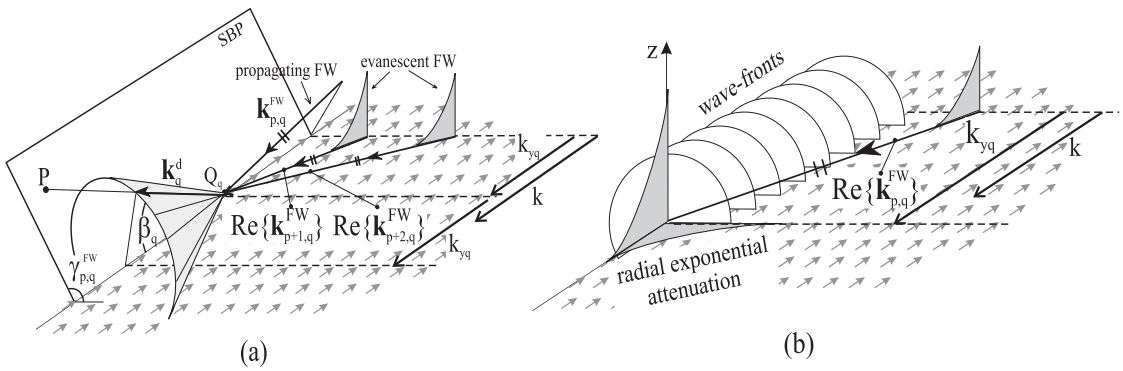

Fig. 2. (a) Propagating diffracted rays along the surface of the diffraction cone centered at Q_q. (b) Evanescent diffracted field excited by evanescent FWs

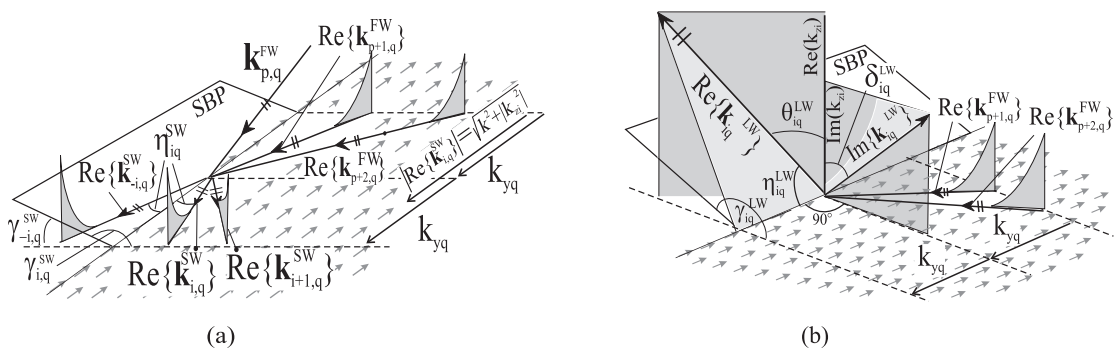

Fig. 3. (a) Propagation paths of the surface wave induced by the q-th FW diffraction at the array edge (b) Direction of real part of the iq-th LW wavenumber. The LW is excited by the q-indexed FWs.

an efficient evaluation of the term $\mathbf{E}_q^d$ in (2) it is convenient to extract some polar singularities thus resulting in an easier integration of the residual part. This extraction is performed via the Wan-der-Waerden technique. As a consequence, we can express $\mathbf{E}_q^d$ as the sum of two terms $\mathbf{E}_q^d = \mathbf{I}_1 + \mathbf{I}_2$. The first term contains the regularized integrand, which becomes smoothly varying around the saddle point and may be approximated by its value at the saddle point γ, thus obtaining

$$\mathbf{I}_1 \approx \sqrt{\frac{2\pi j}{k_{tq} t}} \left[\mathbf{D}_q(\gamma) - \sum_w \frac{\mathbf{r}_{wq}^{GW}}{2\sin\left(\frac{\gamma - \alpha_{wq}^{GW}}{2}\right)} \right] e^{-jk_{tq}t} \tag{3}$$

where α_{wq}^{GW} are the singularities relevant to FW, SW and LW poles, and $\mathbf{r}_{wq}^{GW}$ are the residues associated to these poles. Furthermore $\mathbf{D}_q(\gamma)$ is the integrand in (1), except for the exponential term, calculated at its saddle point, and t is the transverse-to-the-edge direction (Fig. 1). The second term $\mathbf{I}_2$ may be expressed as

$$\mathbf{I}_2 = \sqrt{\frac{2\pi j}{k_{tq} t}} \left[\sum_w \frac{\mathbf{r}_{wq}^{GW}\ F(y^2)}{2\sin\left(\frac{\gamma - \alpha_{wq}^{GW}}{2}\right)} \right] e^{-jk_{tq}t} \tag{4}$$

where $F(y^2)$ is the UTD transition function [1] with $-\frac{3\pi}{2} < arg(y^2) \leq \frac{\pi}{2}$ with argument $y^2 = 2k_{tq}t\sin^2\left(\frac{\gamma-\alpha_{wq}^{GW}}{2}\right)$.

NUMERICAL EXAMPLE

In order to check the accuracy of the asymptotic solution (2), numerical results have been carried out for an array of NxM y-oriented electric dipoles on a grounded dielectric slab. For the purpose of calculation the infinite series in the y-direction has been truncated, thus resulting in $M = 101$ dipoles. Comparisons are made with a reference solution which is constructed via the element-by-element summation of the single dipole source contributions. Fig. 4 shows the y-component of the electric field radiated by the strip array of dipoles with interelement spacing $d_x = 0.7\lambda$ and $d_y = 1.4\lambda$. The dielectric slab is characterized by the thickness $h = 0.2\lambda$ and the relative permittivity $\epsilon_r = 2.2$. Observation are made at the distance $H = 2\lambda$ from the array plane (inset of Fig. 4), at the central M-section of the array itself. It is found that the curve relevant to the present approach very well compare to that for reference solution.

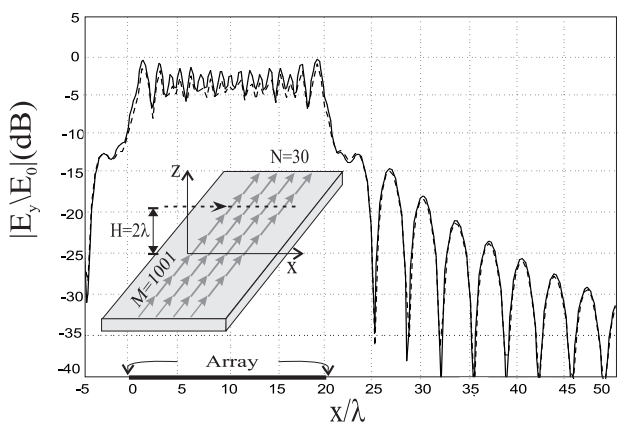

Fig. 4. Normalized electric field of a 30x101 array of dipoles. Calculation are made on a line at the distance $H = 2\lambda$ from the array plane. Element-by-element asymptotics (dashed curve), Global asymptotics (continuous line). Computation times on SUN ULTRASPARC 140 MHz: Element-by-element: 16245 sec; Global asymptotics: 179 sec

REFERENCES

[1] R.G.Kouyoumjian, P.H.Pathak, ”A Uniform Geometrical Theory of Diffraction for an Edge in a perfectly Conducting Surface,” *Proc. IEEE* Vol.62, no.11, pp. 1448-1461 November 1974.

[2] F.Capolino, M.Albani, S.Maci, L.B.Felsen, ”Frequency domain Green’s function for a planar periodic semi-infinite phased array. Part I: truncated Floquet wave formulation, Part II: diffracted wave phenomenology,” *IEEE Trans. Antennas Propagat.*, Vol.47, no. 1, Jan 2000.

[3] F. Capolino, S. Maci and L. B. Felsen, ”Green’s function for a planar phased sectoral array of dipoles,” to be published on RadioScience.

[4] A. Neto, S. Maci, G. Vecchi, M. Sabbadini, ”A truncated Floquet wave diffraction method for the full-wave analysis of large phased arrays. Part I: Basic principles and 2D case, Part II: Generalisation to the 3D case,” *IEEE Trans. Antennas Propagat.*, Vol 48, no.3, March 2000

[5] A. Toccafondi, A.Polemi, S. Maci, ”High frequncy Green’s function for a semi-infinite array of printed dipoles,” *AP conference in Davos*, PP0913, 13-18 April 2000